Abdominal organ motion during inhalation and exhalation breath-holds: pancreatic motion at different lung volumes compared

Lens, Eelco; Gurney-champion, Oliver J.; Tekelenburg, Daniël R.; Van Kesteren, Zdenko; Parkes, Michael; Van Tienhoven, Geertjan; Nederveen, Aart J.; Van Der Horst, Astrid; Bel, Arjan

DOI:
10.1016/j.radonc.2016.09.012

Abdominal organ motion during inhalation and exhalation breath-holds: pancreatic motion at different lung volumes compared – E. Lens *et al.*

Subject characteristics

Table E1: Subject characteristics of the 16 healthy subjects

	Sex	Age (year)	Height (cm)	Weight (kg)	Vital capacity (L)*	Does subject smoke	Expected performance†
1	F	51	163	55	2.7	No	9
2	F	24	176	58	2.1	No	6
3	M	30	180	60	4.3	No	7
4	M	30	175	80	4.0	1 or 2 cigarettes a day	9
5	F	53	158	51	2.1	No	7
6	F	27	170	69	3.5	Occasionally	5
7	F	28	160	38	2.0	No	7
8	F	34	168	75	3.1	Yes	7
9	F	34	170	57	3.1	No	7
10	M	27	184	74	4.5	Recently quit	8
11	F	24	171	60	2.8	No	7
12	M	31	185	77	4.6	No	6
13	M	29	185	84	5.2	Occasionally	6
14	F	28	175	66	3.0	No	5
15	M	24	175	56	3.9	No	8
16	M	31	180	75	3.7	No	7
Group mean		32	173	65	3.4		7

Abbreviations: F = female; M = male.

*We measured the vital capacity of each subject using an analog spirometer (Rudolf Riester GmbH, Jungingen Germany).

†Each subject was asked to score their expected performance on a scale from 1 (stating: "I will not manage") to 10 (stating: "I will manage each breath-hold for 60 s").

2-Dimensional image correlation algorithm

We developed an algorithm in MATLAB (The MathWorks Inc., Natick, MA, USA) that was able to determine the most likely position of a template (i.e. a rectangular region of interest) within all images obtained during a single breath-hold. An example of a breath-holding imaging series is shown in Movie E1, this movie is obtained during a $BH_{70\%}$ of subject 6. The template was defined at the start of breath-holding (i.e. on the first image obtained during that breath-hold) and contained the structure that was being tracked (i.e. pancreatic head or diaphragm). An example of both templates corresponding with Movie E1 is shown in Fig. E1. For each possible template position within each image, the normalized cross-correlation coefficient was calculated and together these formed the correlation surface, which described the probability of all template positions. To achieve sub-pixel resolution, a 2-dimensional Gaussian was fitted to the cross-correlation coefficient values in a 9×9 $pixel^2$ region with the largest value of the correlation surface at the central pixel (pixel size was

$0.93 \times 0.93\ mm^2$). Using this algorithm, we determined the 2-dimensional rigid translation of the template relative to the start of the breath-hold for each of the 100 frames obtained during breath-holding (i.e. the motion during breath-holding).

To improve the accuracy of the obtained motion for each breath-hold, the motion of the pancreatic head during each breath-hold was determined three times with different templates and the obtained results were averaged. The mean absolute difference between the three obtained motion tracks over all subjects in the IS direction obtained from the coronal scans was 0.71 mm (standard deviation: 0.19 mm). The three templates had small differences in size and position around the pancreatic head and were defined on the three different images obtained by averaging two of the first three images of that scan. The template always included the complete pancreatic head as well as a small portion of the liver so that the transition between the pancreas and liver was included. During each breath-hold we visually checked whether the algorithm was able to successfully perform the template matching. To do so, a reference point was placed on an anatomical landmark on the first image. On each subsequent image this reference point was displaced by the same displacement that was obtained for the template and we checked whether this point remained on the selected moving landmark.

The motion of the diaphragm was obtained using the same algorithm with a template with a maximum width of five pixels; the template was placed at the top of the right dome of the diaphragm.

Figure E1: Example of a single coronal MR image at the start of breath-holding for a $BH_{70\%}$ of subject 6. The red rectangles illustrate the templates that were used to obtain the motion of the diaphragm (template 1) and of the pancreatic head (template 2).

Pancreatic motion results of the sagittal slice MRI scans

As mentioned in the Materials and Methods section, we were unable to obtain diaphragm motion from the acquired sagittal slice images. Therefore, we excluded these scans from the analyses in the article. However, to show that the motion data of the pancreas, obtained from the sagittal scans, were similar to the data obtained from the coronal scans, we plotted the obtained pancreatic motion magnitudes and velocities in Figs. E2 and E3. These figures show the pancreatic head motion magnitude in the IS (Fig. E2a) and AP (Fig. E2b) direction and the velocity in the IS direction (Fig. E3), as obtained from the sagittal scans. The motion magnitudes during inhalation breath-holds ($BH_{100\%}$ and $BH_{70\%}$) were larger than during exhalation breath-holds ($BH_{30\%}$ and $BH_{0\%}$); note that these differences can be influenced by differences in breath-hold duration. The organ velocity during the first 10 s of breath-holding was significantly (*P*<0.001) smaller compared with during the remainder of breath-hold for all four different lung volumes. Figure E2a can be compared to Fig. 1b from the main manuscript and Fig. E3 can be compared with Fig. 4a.

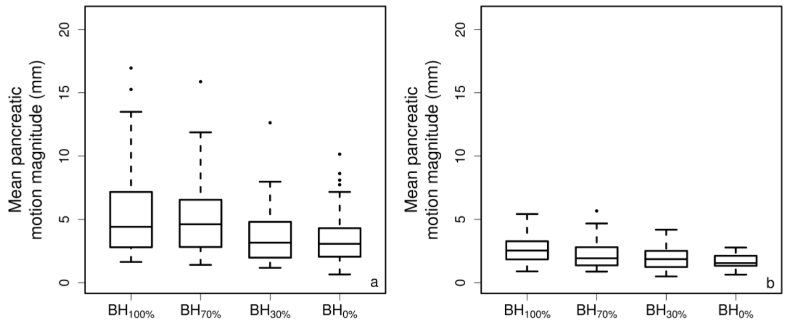

Figure E2: Mean pancreatic motion magnitudes for the four different lung volumes in the inferior-superior direction (a) and anterior-posterior direction (b) during breath-holding in all subjects.

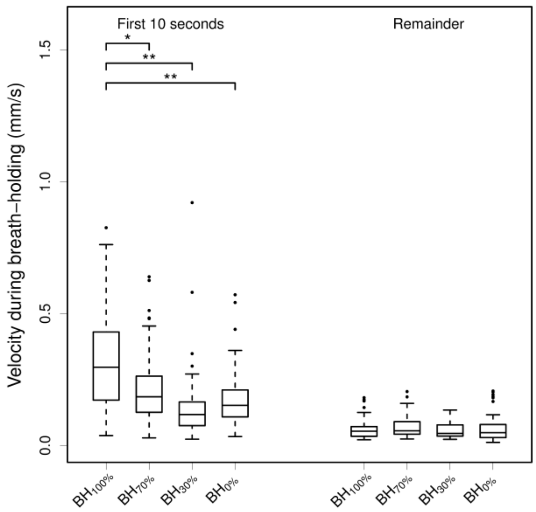

Figure E3: Distributions of pancreatic head velocity in the inferior-superior direction during the first 10 s of breath-holding and during the remainder of the breath-hold for the four lung volumes. Significant differences are indicated by * (0.01<*P*≤0.05) and ** (0.001<*P*≤0.01).